Impurities in synthetic fluorite for deep ultraviolet optical applications

J. Sils,[1,a)] S. Hausfeld,[1] W. Clauß,[2] U. Pahl,[2] R. Lindner,[2] and M. Reichling[1,b)]

[1]*Fachbereich Physik, Universität Osnabrück, Barbarastr. 7, 49076 Osnabrück, Germany*
[2]*Carl Zeiss SMT AG, Rudolf-Eber-Str. 2, 73447 Oberkochen, Germany*

The impurity content of synthetic calciumdifluoride (fluorite, CaF_2) single crystals produced for optical applications in the deep ultraviolet (DUV) and infrared (IR) spectral regions are investigated by luminescence and absorption spectroscopy. Lead, oxygen, and rare earth (RE) ions, namely, trivalent (Ce^{3+}, Pr^{3+}, Sm^{3+}, Eu^{3+}, Gd^{3+}, Tb^{3+}, Dy^{3+}, Ho^{3+}, Er^{3+}, and Yb^{3+}) and divalent (Eu^{2+}) are identified as common impurities. RE ions are dominating impurities in the IR grade sample and the impurity concentration for this sample is found to be about 100 times higher than the one for DUV samples. Due to the strongly reduced RE luminescence background, we additionally identify lead and oxygen in DUV grade crystals. Remarkable differences in the luminescence spectra are found when comparing DUV grade crystals from different sources. © *2009 American Institute of Physics.* [doi:10.1063/1.3224879]

I. INTRODUCTION

The quality of calciumdifluoride (fluorite, CaF_2) as an optical material has been greatly improved over the past years following a demand for highest quality materials used as lens and window material in ultraviolet laser lithography systems.[1] The requirements for the use of CaF_2 in the deep ultraviolet (DUV) spectral region, namely, for lithography at 193 nm, are absolutely stringent and still require tremendous efforts in the growth and preparation of crystals.[2,3] The homogeneity of optical properties and a reduction in the intrinsic birefringence remain major challenges for the implementation of CaF_2 as an optical material for high precision optics in the DUV. The intrinsic birefringence increases dramatically for shorter wavelengths.[4,5] Since it is caused by the anisotropy of the exciton resonance, it is an intrinsic property of the pure material and thus inevitable in applications with short light wavelengths. An additional factor hindering to reach required material properties is the presence of defects such as dislocations[6] and impurities. The concentration and distribution of extrinsic defects in the crystal volume influence the absorption properties and homogeneity of the refractive index. The reduction in the impurity content using chemical scavengers is usually conducted during the growth of the crystal and has significantly improved the optical properties of CaF_2 in the DUV spectral region.[7–9] The impurity content may also play a role for laser damage occurring when irradiating the CaF_2 with UV light at very high fluence. While the laser damage threshold is mainly determined by impurities introduced during polishing for standard surface preparation,[10,11] the damage threshold for crystals prepared by cleavage or by advanced polishing techniques[12] may be determined by step edges,[13–15] surface degradation in air,[16] or finally residual bulk impurities.

In the present work, we investigate the role of residual impurities in nominally pure CaF_2 samples and analyze their relative abundance depending on the commercial quality offered. We compare pure samples with an oxygen doped crystal using a highly sensitive luminescence spectroscopy method and complement our studies with measurements of optical absorption in the UV spectral range.

II. EXPERIMENTAL DETAILS

The samples investigated have been grown by different methods and varied in shape and size from thin 1–2 mm sheets until large monocrystalline blocks of several centimeters in length. Out of a manifold of 23 samples investigated, we select four having representative properties and further on denote these samples as samples A, B, C, and D, respectively. Except for sample B, crystals were grown as an optical material for infrared (IR) or DUV applications. Prior to our investigations, all samples except sample B have been irradiated with 193 nm excimer UV light in multiple pulse modes and pulse energies of 1–5 mJ in the course of other optical testing.

Luminescence was excited quasicontinuously with 5.9 eV photons generated by frequency doubling 100 fs light pulses from a Ti:sapphire laser operated at a repetition rate of 80 MHz. Luminescence light was collected by a lens and focused into quartz fiber connected to a highly sensitive optical multichannel analyzer spectroscopy system based on a LN_2 cooled charge coupled device (CCD) camera. The spectra were acquired over 1000 accumulations of 1 s CCD exposure time each. Two separate measurements were performed for each sample distinguishing the UV and visible ranges by using UV-transparent and UV-nontransparent lenses for collecting luminescence light, respectively. The UV-transparent lens was used for the range of 220–400 nm. The detection at longer wavelengths turned out to be a problem with this lens due to the luminescence of the quartz fiber excited by the scattered UV light. Therefore, we used an UV-nontransparent lens for detection in the range of 370–820 nm. As our experimental setup has not been calibrated to

---
a)Present address: Lissotschenko Mikrooptik GmbH, Bookenburgweg 4-8, 44319 Dortmund, Germany.
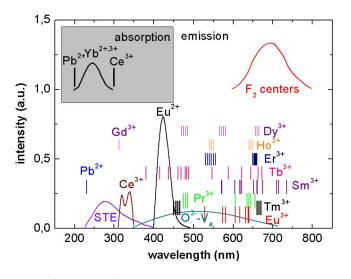b)Electronic mail: reichling@uos.de. Tel.: +49-541-969-2264. FAX: +49-541-969-12264.

FIG. 1. (Color online) Schematic representation of photoluminescence emission and absorption in CaF_2 doped with RE and/or oxygen according to literature data (Ref. 57). Broad bands are shown at their positions with an original width, whereas narrow transitions are represented as vertical lines. Emission and absorption data and their origin are summarized in Table I.

provide values for the absolute fluorescence yield, fluorescence intensities are measured in counts for a variable sampling time but fixed spectral interval. Depending on intensity, fluorescence measurements have been performed with varying sampling time and sensitivity settings of the CCD camera. However, before plotting spectra, we normalized results with respect to sampling time and sensitivity settings so that intensities given in Figs. 2–5 are comparable with each other.

Absorption was measured in the range of 190–400 nm by a commercial UV spectrometer against air as a reference. The oxygen doped sample was annealed at a temperature of 870 K for 15 min prior to the measurement to dissolve possible oxygen defect aggregates and then quenched to room temperature. A more detailed description of the equipment and experimental methods can be found in our earlier work.[17]

III. BACKGROUND

To understand the observed luminescence spectra, it is important to compile spectroscopic information on intrinsic and extrinsic defects found in fluorite that have been identified in literature. Major sources of luminescence can be the self-trapped exciton (STE), F and double F (M) centers created by irradiation with above band gap energy, oxygen defects present in the fluorite lattice, and rare earth (RE) ion impurities. The spectral characteristics of such impurities as reported in literature is discussed below and schematically represented in Fig. 1.

The STE is the primary intrinsic lattice defect created in fluorite under x-ray and vacuum ultraviolet radiations.[18] Electron-hole pairs created by interband transitions relax to the band edges and are localized by strong coupling to the lattice. Upon recombination, luminescence occurs in form of a band of light emission centered at 4.4 eV. The 1 eV width of the band is the result of the strong electron/hole-phonon interaction during restoration of the perfect lattice following the decay of the STE. In our measurements, the intensity of

the 6 eV laser pulses is too weak for a transition across the 11.8 eV band gap of CaF_2 by two-photon absorption that is necessary to create the STE.[19] Another possibility for a band to band excitation in two steps is, however, the presence of unoccupied energy levels in the band gap provided by some impurity. In this case, a much lower light intensity would be sufficient to create electron-hole pairs in a two-step excitation.

The F centers in a virgin crystal are usually created by high energy γ- or x-ray radiation. An association of two F-centers creates an M-center (F_2), which can be found in the [100], [110], and [111] configurations. Experimental work and theory calculations on properties of these centers have been made earlier.[20,21] In CaF_2, a 3.3 eV absorption band of F-centers has been observed,[22] though no luminescence was found at room temperature. The activation energy of the F-center was found to be 1.69 eV, suggesting that F-centers are not mobile in the CaF_2 lattice at room temperature. The comparably small dissociation energy of M-centers (0.31 eV) suggest that they dissociate easily at room temperature. Only M-centers stabilized by Na^+ impurities have been reported to be stable up to 350 K.

Oxygen ions with a neighboring fluorine vacancy incorporated during the growth process form the oxygen defects $O^{2-}V_a$ present in nearly all CaF_2 crystals despite purification efforts.[23] They exhibit a very broad luminescence band centered at 460 nm (2.7 eV) and extending over a wide spectral range of 400–700 nm. An important property of the oxygen defects is to form aggregates at temperatures of 320–420 K as they become mobile and preferably associate in clusters of various sizes and configurations. Once they are formed, the oxygen involved in aggregates becomes nonluminescent in our observed wavelength range. At temperatures of 850–900 K, aggregates dissolve and precipitate as isolated single oxygen defects during subsequent quenching to room temperature.[17]

Common extrinsic defects in CaF_2 are known to be divalent and trivalent RE impurity ions. The luminescence of natural fluorite upon UV excitation was known since 1824 discovered by Mohs.[24] In the 1950s, Feofilov and co-workers[25–36] started a program of systematic research of the absorption and emission properties of RE elements by doping synthetic CaF_2 crystals. The summary of spectroscopic properties of the RE impurities was later compiled in the form of energy level diagrams by Dieke.[37] Görlich *et al.*[38,39] provided an overview of the optical properties of RE in CaF_2 and other ionic crystals using them as active laser materials. A significant contribution in determining the location of energy levels of divalent and trivalent RE in a variety of crystals has later been made by Dorenbos.[40]

Investigations of natural fluorite by x-ray luminescence spectroscopy demonstrated a wide range of RE concentrations and the presence of specific elements strongly depending on the mining site.[41] Each of the elements yields a number of emission lines under x-ray excitation while intrinsic fluorite lattice defects are created by ionizing radiation resulting in complex luminescence spectra. To identify the spectral emission associated with a specific RE impurity, the x-ray luminescence was compared to the luminescence of

synthetically grown crystals doped with one specific RE element and subsequently examined by the x-ray luminescence as well.[41]

In order to clarify the origin of the luminescence found in our samples, we review in the following the most important emission and absorption features of the RE ions of each chemical element and summarize data from different sources in Table I.

A double peak is found for Ce^{3+} emission due to the splitting of the ground state to $^2F_{7/2}$ and $^2F_{5/2}$. The double peak is located at 320 and 340 nm if the excess charge of a trivalent ion is compensated by an interstitial fluorine (type I Ce^{3+} centers).[29,33,42] An O^{2-} substituting fluorine in the nearest neighbor position as a charge compensator (type II Ce^{3+} centers) shift the luminescence to longer wavelengths at 350 and 380 nm.[29,33]

Two groups of Pr^{3+} luminescence lines are found, one centered at 450 nm and the second one in the range between 600 and 700 nm.[31,43] Petit *et al.*[44] reported $^1D_2 \rightarrow {}^3H_4$ and $^1D_2 \rightarrow {}^3H_5$ emission of Pr^{3+} in the ranges of 590–600 nm and 610–615 nm, respectively. Oskam *et al.*[45] reported a multitude of lines between 220 and 800 nm resulting from $^1S_0$ and $4f^15d^1$ emissions upon excitation with 177, 215, and 221 nm light.

The optical properties of Nd^{3+} have been widely investigated because of its good laser properties in many host lattices.[39] In CaF_2, however, only at low temperatures laser operation was possible using the $^4F_{3/2} \rightarrow {}^4I_{11/2}$ emission at 1.06 μm. Despite many absorption bands from the UV to the IR spectral range, only IR luminescence has been observed in most host lattices at room temperature.[31,36]

The Sm^{3+} luminescence is located in the red visible region from 570 to 750 nm wavelength,[31,41,43] whereas Sm^{2+} emits in the range of 700–800 nm.[27,46,47] Taraschan *et al.*[41] assigned lines at 567.5 and 605.5 nm to $^4G_{5/2} \rightarrow {}^6H_{7/2}$ and $^4G_{5/2} \rightarrow {}^6H_{9/2}$ transitions in Sm^{3+} centers of cubic and noncubic symmetries, respectively, which differ by a position of the charge compensating fluorine interstitial with respect to the Sm^{3+} ion in the crystalline lattice.

Eu^{2+} ions emit in a luminescence band centered at 430 nm.[27,48] The slightly asymmetric band covers the spectral range of 400–450 nm. Eu^{3+} emission shows a number of lines in the range of 525–670 nm.[25,26,43]

Gd^{3+} emits in the near UV at 311–314 nm.[31,39,41,43] Upon excitation with 130 nm or lower wavelength light, several strong lines from $5d$-$4f$ luminescence in the VUV spectral range can be observed at low temperature. A similar VUV emission is found for Lu^{3+}.[49]

Tb^{3+} luminescence consists of two sequences of emission lines corresponding to transitions from $^5D_3$ and $^5D_4$ excited states to the $^7F_{6,5,4,3,2,1,0}$ ground state multiplet.[30,31] The wavelength ranges for these sequences are 380–480 and 490–660 nm, respectively, and most intense emission lines are located at 380.2, 414.9, 436.7, and 460.8 nm for the $^5D_3 \rightarrow {}^7F_{6,5,4,3}$ transitions and at 487.8, 546.4, 588.2, and 620.1 nm for the $^5D_4 \rightarrow {}^7F_{6,5,4,3}$ transitions.[30,31]

The groups of Dy^{3+} emission lines are located at 470, 570, 660, 750, and 850 nm.[31,50] The group at 660 nm has been reported to appear also after annealing the crystal in air.[31] With oxygen present in the crystal, Dy^{3+}:O^{2-} luminescence centers are formed having an emission in the red visible spectral range. In oxygen doped samples, they appear as lines at 670 and 675 nm.[41] Dy^{2+} emits in the near IR at 2.3–2.6 μm and the transition $^5I_7 \rightarrow {}^5I_8$ is used for the laser operation.[51]

Ho^{3+} luminescence is composed of several groups of transitions from $^5F_{5,4,3}$ and $^5S_2$ excited states to the ground state split into $^5I_8$ and $^5I_7$ states.[52] Fluorescence lines at 550 and 650 nm for Ho^{3+} have also been reported.[31,43] In natural fluorite Ho^{3+} shows a group of emission lines in the range of 540–560 nm, which are much more intense under x-ray excitation than the Er^{3+} lines located nearby.[41] Ho^{2+} emission shows few lines in the IR spectral range from 1800 to 2000 nm.[35]

Pollack[53] reported several groups of Er^{3+} luminescence lines (primary and secondary) in the range from UV to visible and IR originating from different excited levels. Additional lines are found at 550 and 650 nm.[31,43] Er^{2+} ions can be excited throughout the spectrum from UV to IR in five absorption bands leading to IR luminescence at 2–2.4 μm.[35]

Tm^{3+} ions have only a few very sharp absorption lines and groups of luminescence lines at 460 and 670 nm and in the IR range of 1.7–2 μm.[31,43] Tm^{2+} shows several broad absorption bands between 200 and 700 nm and IR luminescence at 1.0–1.3 μm.[54]

Both Yb^{2+} and Yb^{3+} give rise to absorption in the UV region, Yb^{3+} at 255 nm, Yb^{2+} at 240 and 350 nm, and emit several IR luminescence lines in the range of 890–1036 nm, the strongest one at 974 nm.[28,31] A broad luminescence band at 77 K with a peak at 570 nm was observed.[27] This luminescence is completely thermally quenched already at 120 K and cannot be observed at room temperature.[27]

We did not find any report on Lu^{3+} and Lu^{2+} luminescence in CaF_2. The source of Pb^{2+} in CaF_2 is usually PbF_2 added to remove oxygen from the melt. Arkhangelskaya *et al.*[55] reported on an absorption band at 204 nm and luminescence of Pb^{2+} in CaF_2 at 230 nm.

IV. RESULTS

In our studies, we observe a variety of luminescence features, emission lines, and bands at specific wavelengths over a wide range in the UV and visible spectral regions. Many of them coincide with the data shown in the overview of Fig. 1. None of our investigated samples exhibits all of the emission lines but a rather specific combination of features creates a characteristic luminescence pattern for each crystal that can be regarded as its fingerprint. In the following, we discuss spectra of the selected samples A–D and analyze the luminescence fingerprint of each sample.

Sample A is an IR grade crystal and exhibits the most pronounced line spectrum of all samples examined in this study; its luminescence spectrum is shown in Fig. 2. The spectrum exhibits a number of emissions of RE ions with remarkably high intensity; a pronounced one is the double peak of Ce^{3+} at 320 and 340 nm. From the elevation of the spectrum in the range of 400–450 nm, we anticipate a con-

TABLE I. Summary of the main absorption and luminescence features of RE impurities and oxygen defects in fluorite.

Impurity ion or intrinsic feature	Absorption wavelength (nm)	Emission wavelength (nm)
STE		Broad band at 290[a,b]
F_2 (*M*)-centers	Broad band at 560[c]	Broad band at 690[c]
Pb^{2+}	Narrow bands at 154, 164, and 204[d]	Narrow band at 230
Ce^{3+} type I (ox)	Bands at 220, 330[e,f]	Doublet 350, 380[e,f]
Ce^{3+} type II (int.)	Bands at 240, 310,[e,f] 180, 200, 240, 310[g]	Doublet 320, 340[e,f]
Pr^{3+}		593–598, 610, 614[i]
		Group of lines at 480 and in the range 500–600[j,k]
	Bands between 150 and 200[h]	Many lines between 220 and 800[h]
Nd^{3+}	Bands at ~200, 320, 350, 425, 460, 520, 570, 620, 670, 735, 790, 860, 885[j]	860–870, 910, 1060 (infrared, low temperature)[j,l]
Pm	No stable isotopes	
Sm^{2+}	Bands at 240, 256, 288, 307, 425, 445, line at 690,[m,n] 495, 507, 535, 632[n,o]	Broad band at 750[m]
Sm^{3+}	230, 400[p]	Lines at 567, 571, 572.2, 605.5, 616.7, 617.6, 621.9, 651.6, 660, 661.5, ~675, ~710, ~715, ~735 [j,q,k]
Eu^{2+}	Band at 222 (200–250), several narrow bands in the range 325–400[m]	430 band (400–475)[m,r]
Eu^{3+}	313[s]	528,[t,s,k] 573, 581, 606, 616, 631, 638, 640
Gd^{3+}	Bands at 248, 335[u]	311–314[j,u,q,k]
Tb^{3+}	250–260,[v] ~210 [w]	$^5D_3 \rightarrow {}^7F_{6,5,4,3}$, 380, 415, 437, 461
		$^5D_4 \rightarrow {}^7F_{6,5,4,3}$, 488, 546, 588, 621[x,j]
Dy^{2+}	Bands at 230–490, 580, 720, 910[y,z]	Several lines in the range 2300–2600[z]
Dy^{3+}		Groups of lines at 470, 570, 660, 750 and 850,[y] 480, 570, 660[j]
Ho^{2+}	Bands at 512, 680, 897[aa]	Few lines in the range 1800–2000[aa]
Ho^{3+}	Lines at[ab]	Groups of lines at 540, 650 nm[j,k]
Er^{2+}	Bands at 344, 400, 485, 610, 910[aa]	Several lines in the range 1900–2400[aa]
Er^{3+}		310–320,[ac] 397–403, 466–471, 514–531, 613–621, 756–780, 800–820,
		515–529, 537–553, 830–862, 643–668, 780–803, 957–975, 1400–1520[ac]

TABLE I.   (*Continued.*)

Impurity ion or intrinsic feature	Absorption wavelength (nm)	Emission wavelength (nm)
		Groups at 540 and 650[j] Groups at 530, 550[k]
Tm^{2+}	Bands at 240, 310, 400, 450, 570, and 600[ad]	Several lines and bands in the range of 1000–1300[ad]
Tm^{3+}	Infrared	Groups of lines at 460, 670[j,k]
Yb^{2+}	Band at 260,[ae] narrow band at 365,[m] bands at 230, 360[af]	Broad band at 580 (500–700) only at low temperature[m]
Yb^{3+}	Band at 260[ae]	Several lines in the range 890–1036, the strongest at 973–974[ae,j]
Lu^{2+} and Lu^{3+}	In VUV region[ag]	In VUV region only at low temperature
$O^{2-}V_a$	127, 148, 185[ah]	458[ai,ah]

[a]Reference 63.
[b]Reference 64.
[c]Reference 58.
[d]Reference 55.
[e]Reference 29.
[f]Reference 33.
[g]Reference 42.
[h]Reference 45.
[i]Reference 44.
[j]Reference 31.
[k]Reference 43.
[l]Reference 36.
[m]Reference 27.
[n]Reference 46.
[o]Reference 47.
[p]Reference 65.
[q]Reference 41.
[r]Reference 48.

[s]Reference 26.
[t]Reference 25.
[u]Reference 39.
[v]Reference 66.
[w]Reference 56.
[x]Reference 30.
[y]Reference 50.
[z]Reference 51.
[aa]Reference 35.
[ab]Reference 52.
[ac]Reference 53.
[ad]Reference 54.
[ae]Reference 28.
[af]Reference 34.
[ag]Reference 49.
[ah]Reference 57.
[ai]Reference 17.

tribution from the Eu^{2+} band at 430 nm. The majority of lines between 380 and 500 nm are identified to originate from a Tb^{3+} impurity. According to the excitation spectrum,[56] it is directly excited by our laser line at 212.5 nm and, therefore, shows very strong luminescence. Some weaker lines are located in the range of 530–650 nm. Due to the high intensity of the line emission, the oxygen band luminescence is hidden behind the very strong RE emission. The absorption data taken below 300 nm coincide well with the low energy tail of the oxygen absorption[57] and are indicators of the presence of oxygen in the crystal. The absorption line of Ce^{3+} at 310 nm is clearly visible.

Since oxygen defects play a key role in the use of CaF_2 for DUV applications, we investigate the oxygen doped sample B and compare the results to those obtained from DUV grade samples. Figure 3 shows the respective luminescence spectrum exhibiting a broad band centered at 2.5 eV originating from $O^{2-}V_a$ centers.[57] An additional strong line at 314 nm is associated with a Gd^{3+} emission.[41] This emission is not observed in other crystals we have investigated, which can be explained by the origin of the fluorite material. Taraschan *et al.*[41] found Gd^{3+} emission in natural fluorite originating from specific mining sites in the Baikal lake (Russia) area. Fluorite material from these mining sites has been used for the growth of sample B. Note that the luminescence intensity of this sample due to oxygen defects is three to four orders of magnitudes higher than the luminescence intensity of the other samples. Therefore, RE line emission cannot be detected in the spectrum of Fig. 3 except for the very strong Gd^{3+} emission line.

For the DUV grade sample C, we find the luminescence spectrum shown in Fig. 4 that is remarkably different from the spectra of samples A and B. The sharp lines are similar to those from sample A, however, orders of magnitude lower in intensity. Most of the lines could be identified as transitions of Tb^{3+} as for sample A. The broad band centered at 700 nm is in good agreement with the emission of F_2 centers created by ionizing radiation.[58] The broad feature in the 400–500 nm range is ascribed to $O^{2-}V_a$ centers. Another emission band in the UV range is located at 225 nm accompanied by a strong absorption at 205 nm indicating the presence of Pb^{2+} ions.[55] The presence of Pb^{2+} is probably due to PbF_2 that has been added as a scavenger material during the growth process to remove oxygen. Apparently, the procedure has not been successful in this case. An additional broad absorption band is located at 260 nm and fits well to the one of the Yb^{2+} ions.[34] The luminescence of Yb^{2+} ions is quenched at room temperature, but the absorption is well detectable.
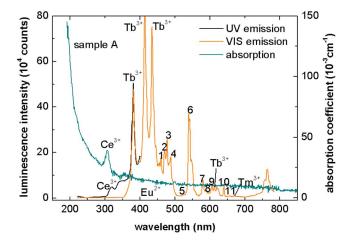
FIG. 2. (Color online) Luminescence of sample A in the UV and visible spectral ranges and the absorption. The numbered lines were identified as emissions of 1-Tb^{3+} or Tm^{3+}, 2-Tb^{3+}, 3-Tb^{3+} or Pr^{3+}, 5-Eu^{3+}, 6-Ho^{3+}, Er^{3+}, or Tb^{3+}, 7-Eu^{3+}, 8-Tb^{3+}, 9-Eu^{3+}, Pr^{3+}, or Sm^{3+}, 10-Eu^{3+}, Sm^{3+}, or Tb^{3+}, and 11-Eu^{3+}, Pr^{3+}, Ho^{3+}, or Tb^{3+}.

FIG. 4. (Color online) Luminescence of sample C in the UV and visible spectral ranges and absorption. An unknown luminescence band observed at 500 nm is marked with a question mark. The numbered lines have been identified as emissions of 1-Tm^{3+}, 2-Tb^{3+}, 3,4-Tb^{3+} or Pr^{3+}, 5-Ho^{3+}, Er^{3+}, or Tb^{3+}, 6-Tb^{3+}, and 7-Eu^{3+}, Pr^{3+}, or Sm^{3+}.

An emission spectrum of sample D is shown in Fig. 5. It is dominated by an intense asymmetric band matching the Eu^{2+} band at 430 nm. Eu^{2+} may easily be introduced into CaF_2 during crystal growth and may be an indication of special growth conditions. However, Eu^{2+} has also deliberately been added to the melt during CaF_2 crystal growth to yield a light conversion material shifting the wavelength from the UV spectral region to blue.[59,60] A number of narrow lines interlace the spectrum over the entire measured wavelength range. Tb^{3+} lines are present in the range of 380–500 nm, which like in the case of samples A and C originate from transitions from the $^5D_3$ excited state to the ^7F ground multiplet. We observe weaker Tb^{3+} emission also from the $^5D_4$ state. The rest of the emission lines belong most probably to Er^{3+}, Ho^{3+}, and Dy^{3+} ions. The intensity of the spectral lines for sample D is smaller than for sample C and thus the smallest of all measured samples. There is no indication for F_2 centers but we anticipate a small contribution from $O^{2-}V_a$ defects.

V. DISCUSSION AND CONCLUSIONS

Apart from the oxygen doped sample B, the dominating luminescence features in all fluorite samples investigated are found to belong to RE impurities mostly in their RE^{3+} charge state. This is in line with reports in literature where it has been shown that RE^{2+} ions are stable only if the ground state of the RE^{2+} ion is well below the edge of the conduction band.[40] Charge transfer in the form of capturing an excited valence band electron by a RE^{3+} ion is required to convert a RE^{3+} ion into a RE^{2+} ion. Thus we consider most of RE ions being in the RE^{3+} state in an as-prepared crystal. Sample A contains two orders of magnitude larger concentrations of RE elements than samples C and D. This sample is specified for use in the IR spectral range where larger concentrations of RE are not critical since the strongest absorption bands of most RE^{3+} are located in the UV and DUV ranges. The spectrum of the oxygen doped sample B is naturally dominated by the oxygen emission feature located at 400–500 nm and
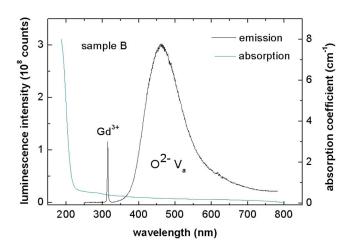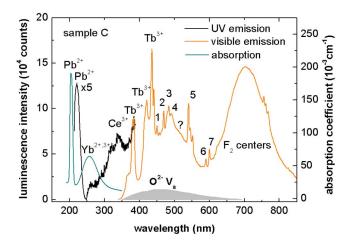

FIG. 3. (Color online) Luminescence and absorption of the oxygen doped sample B exhibiting the oxygen defect band centered at 460 nm and a Gd^{3+} line at 314 nm.
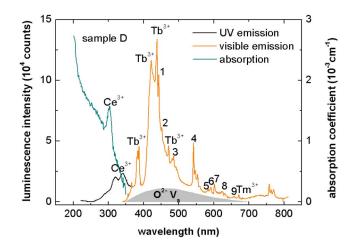

FIG. 5. (Color online) Luminescence of sample D in the UV and visible spectral ranges and Absorption . Numbered luminescence lines are identified as emissions from 1,2-Tm^{3+}, 3-Tb^{3+} or Pr^{3+}, 4-Ho^{3+}, Er^{3+} or Tb^{3+}, 5-Eu^{3+}, 6-Tb^{3+}, 7-Eu^{3+}, Pr^{3+}, or Sm^{3+}, 8-Sm^{3+}, or Tb^{3+}, and 9-Pr^{3+}, Er^{3+}, Dy^{3+}, or Tm^{3+}.

we determined an oxygen concentration of (2100 ± 632) ppm using absorption data.[61] Our apparatus does not allow the determination of absolute concentrations of impurities. However, from a comparison of luminescence intensities of nominally pure samples to the oxygen doped sample, we can derive as a very rough estimate that RE concentrations for DUV grade samples are in the range of some ppm.

The investigation of charge transfer phenomena shows that high energy photons[40] or γ- or x-ray irradiation is required for the creation of RE^{2+} ions from RE^{3+} ions.[32] This process is accompanied by a dramatic change in the optical properties switching the sharp spectral lines of absorption and luminescence of the RE^{3+} ions to broad, bandlike spectra of the RE^{2+} ions. The reason for that is the location of the ground states of most divalent RE ions just below the bottom of the conduction band.[40] The emission resulting from RE^{2+} excited states intersecting with the states of the conduction band over a wide energy range leads to a broad band emission. However, as noted before, divalent RE ions are stable only under certain conditions. The charge transfer process was found to be easily reversible by heating the crystal or irradiating RE^{2+} ions in their absorption bands. The dominance of RE^{3+} is reflected in our experimental results for samples A, C, and D exhibiting only two features ascribed to divalent impurities, namely, the Eu^{2+} emission band at 430 nm present in all samples and Yb^{2+} absorption at 260 nm for sample C. A possible explanation for this finding is the prehistory of the samples that have been irradiated by excimer light. This irradiation may have caused the creation of Eu^{2+} and Yb^{2+} from the trivalent ions by the described charge transfer transition. These two impurities are more stable against backconvertion to the trivalent form, as their electronic ground states are located deeper in the bandgap than that of the other RE^{2+} species.[40]

From the luminescence spectra of our samples, we can undoubtedly identify Ce^{3+}, Tb^{3+}, Gd^{3+}, and Eu^{2+} impurities. The less intensive emissions of Dy^{3+}, Ho^{3+}, Sm^{3+}, Er^{3+}, Tm^{3+}, and Pr^{3+} located in the 550–800 nm range strongly overlap, and with our equipment we could not identify them to belong to one specific element. We are not able to draw any conclusions about Pm^{3+} and Lu^{3+} ions. Pm has no stable isotopes and our literature research provided no matches for Lu luminescence in CaF_2 as well as there are no data about Lu in review articles of Görlich *et al.*[39] and Feofilov.[31,62] Yb^{2+} and Nd^{3+} luminescences are fully quenched at room temperature[27,39] and therefore, it is not present in our spectra. Specific impurities such as Gd^{3+} and Pb^{2+} are found in samples B and C, respectively. They originate from the mining site of the raw material like for sample B (Ref. 41) or specific treatment during the crystal growth, for example, adding PbF_2 to remove oxygen from the melt as for sample C. The latter shows both emission and absorption of the Pb^{2+} centers allowing for a clear identification. The absorption band at 260 nm coincides with the Yb^{2+} absorption reported in Ref. 34 and the broad emission band at 700 nm fits well to the luminescence originating from F_2 centers created by x-ray and γ-irradiations.[58]

As a result of purification during the crystal growth,

samples C and D have been designed as suitable for DUV applications and contain only small residual concentrations of impurities, which are mostly RE ions. No stringent evidence for oxygen contamination can be presented for samples C and D. However, as the RE luminescence intensity is drastically smaller than for sample A, the elevation of the spectrum from the zero line observed over the whole visible range indicates the presence of a broad background signal coinciding with a feature expected for oxygen luminescence. We suggest that there is a small residual concentration of single oxygen defects present in these samples as indicated in Figs. 4 and 5.

Earlier investigations show that Ce^{3+} forms two types of defect centers in CaF_2. For the type I centers, O^{2-} replaces next neighbored fluorine in the [111] direction for charge compensation and associated luminescence peaks are located at 350 and 380 nm.[33] For the type II Ce^{3+}-centers,[33] interstitial fluorine is the charge compensator and the double peak shifts to shorter wavelengths. The maxima are located at 320 and 340 nm for the type II centers. The position of Ce^{3+} peaks at these wavelengths in Figs. 2–5 suggests that mostly type II Ce^{3+}-centers are present in the samples investigated.

In the following, we discuss the reasons for the presence of only specific element emissions in our spectra. Besides RE ions clearly identified in our study due to their intense emission, RE ions such as Er^{3+}, Nd^{3+}, Pr^{3+}, and Eu^{3+} have been found in fluorite by Taraschan *et al.*[41] using x-ray excitation spectroscopy. Contrary to these results, no strong emission of the specified elements was found in our samples or the emission of them could not clearly be identified due to an overlap of emissions in the visible spectral range. A number of narrow Er^{3+}, Nd^{3+}, Pr^{3+}, and Eu^{3+} absorption lines in the visible part of the spectrum cannot be excited with our laser system. Another reason possibly explaining the absence of specific ions is thermal quenching of the luminescence. As noted before, luminescence is completely quenched for Yb^{2+} and Sm^{2+} ions at 200 and 280 K,[27] respectively, whereas for Eu^{2+} at 430 K. At room temperature, Eu^{2+} still emits at maximum intensity and can be observed as the luminescence band at 430 nm for samples A, C, and D in Figs. 2–5. Nd^{3+} has been widely investigated in various host lattices as an activator for laser materials. In CaF_2 only at low temperature laser generation could be achieved while excited levels are thermally quenched at room temperature. We believe that this is the reason why we cannot identify Nd^{3+} luminescence in our samples. It is also known that divalent RE ions are even more sensitive to thermal quenching than the trivalent ones.[40] Therefore, it is likely that the luminescence of RE^{2+} is quenched for most of the elements and the luminescence spectra consist mainly of the trivalent RE emissions.

In summary, we have shown that UV laser light excited luminescence is a most sensitive method to detect and identify most of the extrinsic defects present in fluorite samples. An extension to other excitation wavelengths and luminescence detection at low temperature to avoid quenching would allow one to cover all possible defects. Apparently, a detection sensitivity for RE impurities in the ppm range could be achieved for the DUV grade samples available for the present study. However, the method applied is clearly

capable of detecting much smaller amounts of trace impurities that may be reached in the future by further efforts in purification during crystal growth.

ACKNOWLEDGMENTS

[1] M. Rothschild, T. M. Bloomstein, J. E. Curtin, D. K. Downs, T. H. Fedynyshyn, D. E. Hardy, R. R. Kunz, V. Liberman, J. H. C. Sedlacek, R. S. Uttaro, A. K. Bates, and C. Van Peski, J. Vac. Sci. Technol. B **17**, 3262 (1999).

[2] M. Letz, A. Engel, W. Mannstadt, L. Parthier, U. Natura, and K. Knapp, Proc. SPIE **5377**, 1797 (2004).

[3] K. A. Bates, M. Rothschild, T. M. Bloomstein, T. H. Fedynyshyn, R. R. Kunz, V. Liberman, and M. Switkes, IBM J. Res. Dev. **45**, 605 (2001).

[4] J. H. Burnett, Z. H. Levine, and E. L. Shirley, Phys. Rev. B **64**, 241102 (2001).

[5] J. H. Burnett, Z. H. Levine, and E. L. Shirley, Photonics Spectra **35**, 88 (2001).

[6] A. M. Stoneham, Semicond. Sci. Technol. **17**, L15 (2002).

[7] T. Oba, Nippon Kessho Gakkaishi **31**, 238 (2004).

[8] C. Görling, U. Leinhos, and K. Mann, Opt. Commun. **249**, 319 (2005).

[9] J. T. Mouchovski, K. A. Temelkov, N. K. Vuchkov, and N. V. Sabotinov, J. Phys. D **40**, 7682 (2007).

[10] S. Gogoll, E. Stenzel, M. Reichling, H. Johansen, and E. Matthias, Appl. Surf. Sci. **96–98**, 332 (1996).

[11] S. Gogoll, E. Stenzel, H. Johansen, M. Reichling, and E. Matthias, Nucl. Instrum. Methods Phys. Res. B **116**, 279 (1996).

[12] J. Sils, M. Reichling, E. Matthias, and H. Johansen, Czech. J. Phys. **49**, 1737 (1999).

[13] A. V. Puchina, V. E. Puchin, M. Huisinga, R. Bennewitz, and M. Reichling, Surf. Sci. **402–404**, 687 (1998).

[14] C. Barth and M. Reichling, Surf. Sci. **470**, L99 (2000).

[15] V. E. Puchin, A. V. Puchina, M. Huisinga, and M. Reichling, J. Phys.: Condens. Matter **13**, 2081 (2001).

[16] M. Reichling, M. Huisinga, S. Gogoll, and C. Barth, Surf. Sci. **439**, 181 (1999).

[17] J. Sils, E. Radzhabov, and M. Reichling, J. Phys. Chem. Solids **68**, 420 (2007).

[18] A. K. S. Song and R. T. Williams, *Self-Trapped Excitons*, 2nd ed. (Springer, Berlin, 1996).

[19] R. Lindner, M. Reichling, R. T. Williams, and E. Matthias, J. Phys.: Condens. Matter **13**, 2339 (2001).

[20] A. V. Puchina, V. E. Puchin, E. A. Kotomin, and M. Reichling, Solid State Commun. **106**, 285 (1998).

[21] Y. Ma and M. Rohlfing, Phys. Rev. B **77**, 115118 (2008).

[22] K. Atobe, J. Chem. Phys. **71**, 2588 (1979).

[23] J. T. Mouhovski, Prog. Cryst. Growth Charact. Mater. **53**, 79 (2007).

[24] http://de.wikipedia.org/wiki/Fluorit (in German).

[25] P. P. Feofilov, Dokl. Akad. Nauk SSSR **99**, 975 (1954).

[26] P. P. Feofilov, Dokl. Akad. Nauk SSSR **99**, 731 (1954).

[27] P. P. Feofilov, Opt. Spektrosk. **1**, 992 (1956).

[28] P. P. Feofilov, Opt. Spektrosk. **5**, 216 (1958).

[29] P. P. Feofilov, Optika i Spektroskopiya **6**, 234 (1959).

[30] P. P. Feofilov, Opt. Spektrosk. **10**, 142 (1961).

[31] P. P. Feofilov, Izv. Akad. Nauk SSSR, Ser. Fiz. **26**, 435 (1962).

[32] P. P. Feofilov, Opt. Spektrosk. **12**, 531 (1962).

[33] A. A. Kaplyanskii, V. N. Medvedev, and P. P. Feofilov, Opt. Spektrosk. **14**, 664 (1963).

[34] A. A. Kapylanskii and P. P. Feofilov, Opt. Spektrosk. **13**, 235 (1962).

[35] Y. E. Kariss and P. P. Feofilov, Opt. Spektrosk. **15**, 572 (1963).

[36] Y. E. Kariss, M. N. Tolstoi, and P. P. Feofilov, Opt. Spektrosk. **18**, 440 (1965).

[37] G. H. Dieke, *Spectra and Energy Levels of Rare Earth Ions in Crystals*, edited by H. M. Crosswhite and H. Crosswhite (Interscience Publishers, New York, 1968).

[38] I. P. Görlich, H. Karras, G. Koetitz, and R. Lehmann, Phys. Status Solidi **5**, 437 (1964).

[39] P. Görlich, H. Karras, G. Kötitz, and R. Lehmann, Phys. Status Solidi **6**, 277 (1964).

[40] P. Dorenbos, J. Phys.: Condens. Matter **15**, 8417 (2003).

[41] A. N. Tarashchan, O. A. Krasil'shchikova, and A. N. Platonov, Konstitutsiya i Svoistva Mineralov **9**, 111 (1975).

[42] G. J. Pogatshnik and D. S. Hamilton, Phys. Rev. B **36**, 8251 (1987).

[43] I. V. Stepanov and P. P. Feofilov, Dokl. Akad. Nauk SSSR **108**, 615 (1956).

[44] R. H. Petit, P. Evesque, and J. Duran, J. Phys. C **14**, 5081 (1981).

[45] K. D. Oskam, A. J. Houtepen, and A. Meijerink, J. Lumin. **97**, 107 (2002).

[46] W. Kaiser, C. G. B. Garrett, and D. L. Wood, Phys. Rev. **123**, 766 (1961).

[47] P. P. Sorokin and M. J. Stevenson, IBM J. Res. Dev. **5**, 56 (1961).

[48] Y. B. Vladimirskii, G. M. Zakharov, T. I. Nikitinskaya, V. M. Reiterov, and P. A. Rodnyi, Opt. Spektrosk. **32**, 756 (1972).

[49] V. N. Makhov, S. K. Batygov, L. N. Dmitruk, M. Kirm, S. Vielhauer, and G. Stryganyuk, Phys. Solid State **50**, 1625 (2008).

[50] A. Sivaram, H. Jagannath, D. R. Rao, and P. Venkateswarlu, J. Phys. Chem. Solids **40**, 1007 (1979).

[51] L. F. Johnson, Proc. IRE **50**, 1691 (1962).

[52] M. B. Seelbinder and J. C. Wright, Phys. Rev. B **20**, 4308 (1979).

[53] S. A. Pollack, J. Chem. Phys. **38**, 2521 (1963).

[54] Z. J. Kiss, Phys. Rev. **127**, 718 (1962).

[55] V. A. Arkhangel'skaya, V. M. Reiterov, and L. M. Trofimova, J. Appl. Spectrosc. **32**, 67 (1980).

[56] K. V. Ivanovskikh, V. A. Pustovarov, B. V. Shul'gin, and M. Kirm, Russ. Phys. J. **48**, 984 (2005).

[57] E. Radzhabov and P. Figura, Phys. Status Solidi B **136**, K55 (1986).

[58] G. A. Tishchenko and P. P. Feofilov, Bull. Acad. Sci. USSR, Phys. Ser. (Engl. Transl.) **20**, 440 (1956).

[59] H. Nagayoshi, S. Nishimura, and K. Terashima, Conference Record of the 2006 IEEE Fourth World Conference on Photovoltaic Energy Conversion, 2006 (unpublished), Vol. 1, pp. 150–153.

[60] S. Nishimura, K. Terashima, and H. Nagayoshi, J. Appl. Phys. **104**, 053103 (2008).

[61] A. Molchanov, J. Friedrich, G. Wehrhan, and G. Müller, J. Cryst. Growth **273**, 629 (2005).

[62] P. P. Feofilov, *Spektroskopija Kristallov* (Nauka, Moscow, 1966), p. 87.

[63] R. T. Williams and K. S. Song, J. Phys. Chem. Solids **51**, 679 (1990).

[64] R. Lindner, R. T. Williams, and M. Reichling, Phys. Rev. B **63**, 075110 (2001).

[65] J. R. O'Connor and H. A. Bostick, J. Appl. Phys. **33**, 1868 (1962).

[66] W. Viehmann, J. Chem. Phys. **47**, 875 (1967).